AIP | Applied Physics Letters

A micro seismometer based on molecular electronic transducer technology for planetary exploration

Hai Huang, Bryce Carande, Rui Tang, Jonathan Oiler, Dmitri Zaitsev, Vadim Agafonov, and Hongyu Yu

Citation: Applied Physics Letters **102**, 193512 (2013); doi: 10.1063/1.4806983
View online: http://dx.doi.org/10.1063/1.4806983
View Table of Contents: http://scitation.aip.org/content/aip/journal/apl/102/19?ver=pdfcov
Published by the AIP Publishing

Articles you may be interested in

Feedback cooling of cantilever motion using a quantum point contact transducer
Appl. Phys. Lett. **101**, 133104 (2012); 10.1063/1.4754606

Towards a lowpower miniaturized micromechanical electronic nose
AIP Conf. Proc. **1362**, 247 (2011); 10.1063/1.3626377

Super-rolloff electron tunneling transduction of nanomechanical motion using frequency downmixing
Appl. Phys. Lett. **97**, 253108 (2010); 10.1063/1.3527931

Simple force balance accelerometer/seismometer based on a tuning fork displacement sensor
Rev. Sci. Instrum. **75**, 3045 (2004); 10.1063/1.1786333

Cantilever transducers as a platform for chemical and biological sensors
Rev. Sci. Instrum. **75**, 2229 (2004); 10.1063/1.1763252

This article is copyrighted as indicated in the article. Reuse of AIP content is subject to the terms at: http://scitation.aip.org/termsconditions. Downloaded to IP: 129.219.247.33 On: Mon, 09 Feb 2015 02:58:34

A micro seismometer based on molecular electronic transducer technology for planetary exploration

Hai Huang,[1] Bryce Carande,[2] Rui Tang,[1] Jonathan Oiler,[2] Dmitri Zaitsev,[3] Vadim Agafonov,[3] and Hongyu Yu[1,2]
[1]*School of Electrical, Computer and Energy Engineering, Arizona State University, Tempe, Arizona 85287, USA*
[2]*School of Earth and Space Exploration, Arizona State University, Tempe, Arizona 85287, USA*
[3]*Center of Molecular Electronics, Moscow Institute of Physics and Technology, Moscow, Russia*

(Received 1 March 2013; accepted 2 May 2013; published online 16 May 2013)

This letter describes an implementation of micromachined seismometer based on molecular electronic transducer (MET) technology. As opposed to a solid inertial mass, MET seismometer senses the movement of liquid electrolyte relative to fixed electrodes. The employment of micro-electro-mechanical systems techniques reduces the internal size of the sensing cell to 1 μm and improves the reproducibility of the device. For operating bias of 600 mV, a sensitivity of 809 $V/(m/s^2)$ was measured under acceleration of 400 $\mu g(g \equiv 9.81\,m/s^2)$ at 0.32 Hz. A -115 dB (relative to $(m/s^2)/\sqrt{Hz}$) noise level at 1 Hz was achieved. This work develops an alternative paradigm of seismic sensing device with small size, high sensitivity, low noise floor, high shock tolerance, and independence of installation angle, which is promising for next generation seismometers for planetary exploration. © *2013 AIP Publishing LLC*.
[http://dx.doi.org/10.1063/1.4806983]

Planetary seismology, the study of how seismic waves propagate within a planet, is particularly useful in determining its interior structure and composition. Much is known about the Earth's interior, thanks to advanced seismic instruments. Comparatively, little is known about the interiors of other terrestrial planets due to the difficulties in both instrument development and deployment. A planetary seismometer must first satisfy typical planetary instrumentation requirements, such as small size, low power consumption, and robust operation. Second, other terrestrial planets like Moon and Mars are expected to have much lower seismicity than Earth, meaning that the seismic signals of interest will be comparatively weak.[1] Therefore, low self-noise is a critical parameter for planetary seismometers. Furthermore, since planetary seismometers may experience a high deceleration as they land, they must be able to withstand very high shocks.[2] Traditional wide-band spring-mass based seismometers are large, heavy, fragile, power-hungry, and most importantly require complicated installation due to the use of large solid suspended proof masses for thermal self-noise reduction.[3] Also, accurate installation is strictly required to ensure good ground coupling and alignment to the gravity direction. Capacitive solid-state spring-mass system based micro seismometers have been developed using Micro-Electro-Mechanical Systems (MEMS) processes to reduce the size of the traditional designs.[4] They have limited successes because of the fragility and the inherent limitation of working mechanism of the solid-state mass-spring system, which still requires strict installation angle.[5]

Different from solid-state seismometers, seismometers based on molecular electronic transducer (MET) technology sense the movement of a liquid electrolyte between electrodes by converting it to electrical current. Commercially available MET seismometer uses standard machined platinum (Pt) mesh as electrodes and plastic grids as dielectric inter-electrode spacers for the sensing element,[6] leading to low reproducibility and limitation on performance optimization. MEMS techniques have been introduced to build the MET sensing element by He (Ref. 7) and Li (Ref. 8). However, their devices suffer from difficulties of alignment of the channels in stacked wafers and still have large internal dimensions, which limit the performance. Recently, an alternative approach to develop MEMS MET seismometer was reported with preliminary results,[9] where the inter-electrode distance of the device was scaled down to 1 μm, resulting in significant improvement of sensitivity and noise. This letter provides the theoretical analysis of the device physics, which is verified by systematically conducted experiments for complete characterization of the device including linearity, sensitivity, and noise. The advantages of micro seismometer by combining MEMS and MET technology include small size, high shock tolerance by eliminating fragile suspended components, high sensitivity especially at low frequencies, and low self-noise.

The core component in the micro MET seismometer is the molecular electronic cell, as diagramed by Fig. 1. Four electrodes (Pt) configured as anode-cathode-cathode-anode (ACCA), separated by silicon nitride (SiN) dielectric spacers, span the width of channels filled with an electrolyte containing iodide ions. Holes through the electrodes and dielectric spacers allow fluid to flow through the channels. The ends of the channel are capped by high-flexibility rubber diaphragms, allowing the fluid to behave inertially. Fig. 2 details the microfabrication processes. A silicon wafer with low pressure chemical vapor deposited (LPCVD) SiN layer on top forms the substrate of the device. The four electrodes are 20 nm/200 nm Ti/Pt layers patterned by photolithography and deposited by E-beam evaporation and followed by lift-off. Platinum is chosen as the electrodes because it is conductive yet chemically inert to the electrolyte. Each electrode is separated by a 1 μm plasma enhanced chemical vapour

 © 2013 AIP Publishing LLC

This article is copyrighted as indicated in the article. Reuse of AIP content is subject to the terms at: http://scitation.aip.org/termsconditions. Downloaded to IP: 129.219.247.33 On: Mon, 09 Feb 2015 02:58:34

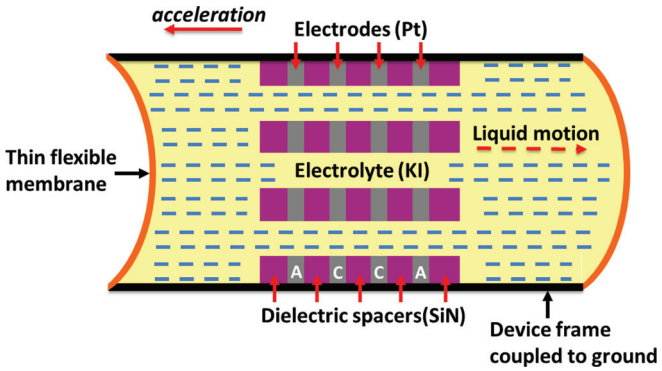

FIG. 1. The schematic view of MET seismometer sensing element.

deposited (PECVD) SiN layer processed at 350 °C and branches to a separate contact pad used for electrical connection to the external circuitry. An additional gold (Au) layer at the connecting wire and pad region is deposited to increase the electrical conductivity. Finally, deep reactive ion etching (DRIE) is used to etch the backside silicon. The DRIE stops as the reactive agents reach the bottom LPCVD SiN layer, leaving a thin diaphragm with a thickness of 5.8μm. After that a focused ion beam (FIB) system (Nova 200 NanoLab, FEI) is used to mill the through holes from front side on the diaphragm to form the channels, exposing sidewall electrodes to the electrolyte that fills the channel. Scanning electron microscope (SEM) images of a through hole milled by FIB on the 5.8μm thin diaphragm and its well-aligned and smooth side wall showing exposed alternating Pt and SiN layers are shown in Figs. 2(h) and 2(i), respectively.

Each anode-cathode pair in the cell is actually an electrochemical cell. When the electrodes are biased, reversible chemical reactions transfer charges between anode and cathode via ions in the electrolyte. Therefore, an electrical path is established. Without fluid motion, diffusion is the only mechanism to transport the ions in solution. A symmetric pattern of ion concentration and its gradient develops, with each ion species having the highest concentration near the electrodes that produces it, and being most depleted near the opposite electrodes.[10] In the presence of an external ground

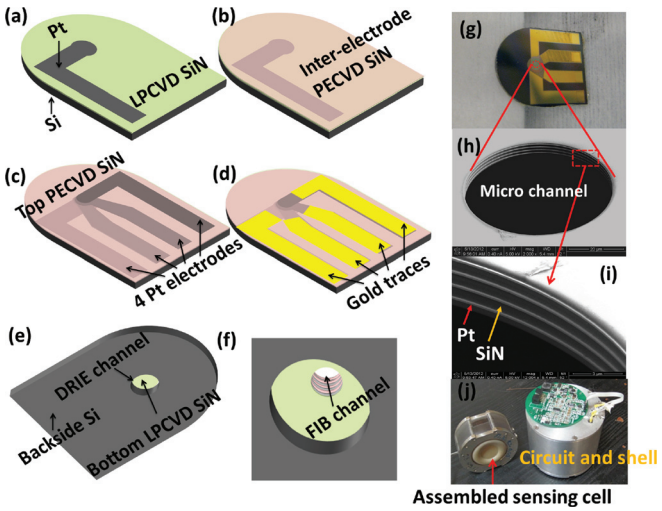

FIG. 2. The fabrication processes of the micro MET seismometer core sensing element (a)-(f) and fabricated and packaged device (g)-(j).

acceleration pointing to the left (Fig. 1), an inertial driving force is applied on the liquid electrolyte. The electrolyte moves to the right along the channel once the driving force exceeds the hydrodynamic drag force. Let $u(t)$ be the ground motion along the channel and $x(t)$ the displacement of the liquid inertial mass relative to the ground, both positive to the right. There are two real forces acting on the mass:

a. Restoring force from the flexible membrane, $-kV(t)$, negative since it opposes the flow motion, where $V(t)$ is the volume of fluid passing through the channel, k is the coefficient of volume stiffness and depends only on the characteristics of the membrane.[11]
b. Damping force, $-R_h S_{ch} dV(t)/dt$, which is linearly proportional to the volumetric flow rate of the liquid associated with the hydrodynamic resistance R_h and is negative since it also opposes the flow motion. The acceleration of the mass relative to an inertial reference frame will be the sum of the acceleration with respect to the ground $d^2x(t)/dt^2$ and the ground acceleration $a(t) = d^2u(t)/dt^2$. Since the sum of forces must be equal to the mass times the acceleration, the equation that governs the motion of the liquid can therefore be expressed as

$$-R_h S_{ch} \frac{dV(t)}{dt} - kV(t) = m\frac{d^2x(t)}{dt^2} + ma(t), \tag{1}$$

with the relations of

$$V(t) = S_{ch}x(t), m = \rho L S_{ch}, \tag{2}$$

where m is the mass of the electrolyte, ρ is the density of the electrolyte, S_{ch} is the cross-section area of the channel, and L represents the channel length. By changing variable of $Q(t) = dV(t)/dt$, where $Q(t)$ is the volumetric flow rate, Eq. (1) can be transformed to frequency domain. So the magnitude of the transfer function of mechanical system in MET cell configured in Fig. 1 in frequency domain can be obtained as follows:

$$|H_{mech}(\omega)| = \frac{|Q(\omega)|}{|a(\omega)|} = \frac{\rho L}{\sqrt{\left(\frac{\rho L}{S_{ch}}\right)^2 \frac{(\omega^2 - \omega_0^2)^2}{\omega^2} + R_h^2}}, \tag{3}$$

where $\omega_0 = \sqrt{k/\rho L}$ is the mechanical resonant frequency of the device. Due to the movement of the electrolyte relative to the frame, besides diffusion, an additional convective transport of ions between the electrodes occurs, which produces unsymmetrical pattern of ion concentration and leads to a significant change in the concentration gradient near the electrode surface, and thereby a change in the output current through the electrodes. The output signal is the amplitude of the differential cathode current.[10,12] An analytical approximation of the electrochemical transfer function in frequency domain is[13,14]

$$|H_{ec}(\omega)| \sim \frac{1}{\sqrt{1 + \left(\frac{\omega}{\omega_D}\right)^2}}, \tag{4}$$

This article is copyrighted as indicated in the article. Reuse of AIP content is subject to the terms at: http://scitation.aip.org/termsconditions. Downloaded to IP: 129.219.247.33 On: Mon, 09 Feb 2015 02:58:34

where $\omega_D = D/d^2$ is the diffusion frequency, D is diffusion coefficient, and d is the inter-electrode distance. The overall frequency-dependent transfer function of a MET seismometer is a superposition of the transfer functions of the mechanical and electrochemical system, which can be written as

$$|H(\omega)| \sim \frac{\rho L}{\sqrt{\left(\frac{\rho L}{S_{ch}}\right)^2 \frac{(\omega^2-\omega_0^2)^2}{\omega^2} + R_h^2}} \frac{1}{\sqrt{1+\left(\frac{\omega}{\omega_D}\right)^2}}. \quad (5)$$

It can be seen from Eq. (5) that there are two poles in the transfer function: ω_0 and ω_D. Practically, for a MET seismometer, $\omega_0 < \omega_D$. Therefore, the low cutoff frequency is determined by ω_0, and the high cutoff frequency is determined by ω_D. One of the most significant advantages of this work is the capability to create the MET cell with inter-electrode distance (d) down to 1μm by MEMS techniques, which is more than two orders of magnitude smaller than is possible for known mesh-based devices (200–300 μm). As a result, ω_D increases significantly. Specifically in our device, $d = 1\mu$m, $D = 2 \times 10^{-9}\text{m}^2/\text{s}, \omega_D = 2\text{kHz}$. In other words, scaling down of d moves the second pole of the system transfer function to the right of the frequency axis, leading to broadening in bandwidth.

The chip with sensing cell is placed between two plastic housing, having a passing through channel. Ends of the channel were covered with flexible chemically inert rubber membranes. All assemble is pressed between two metal flanges. The junctions between chip and plastic parts are sealed with soft O-rings. The electrolyte is filled using vacuum method. The packaged device is assembled inside an air protecting shell. The whole assembly is shown in Fig. 2(j). The cell output signal is measured by an amplification circuit consisting of two transimpedance amplifiers which convert current signals from two cathodes to voltage with a conversion coefficient of 100 kΩ and followed by a differential amplifier which transforms the difference between the two converted signals into output voltage. The testing assembly is then placed on the motion exciter and frequency response has been determined using harmonic scan method. The devices under test are sequentially subjected to a series of excitations whose amplitudes are constant in acceleration units and the frequencies cover the range of interest (0.08–80 Hz). In units of Earth's surface gravity ($g \equiv 9.81\text{m}/\text{s}^2$), the excitation amplitude is 400μg in the long period range (0.08–8 Hz) and 1000μg in the short period range (12–80 Hz). Fig. 3 shows the sensitivity frequency response curves for a single-50 μm diameter-channel device under different bias voltages. Under a bias voltage of 600 mV, the sensitivity reaches $809\text{V}/(\text{m}/\text{s}^2)$ at 0.32 Hz, and is greater than $100\text{V}/(\text{m}/\text{s}^2)$ over frequency range of 0.08–16 Hz.

The linearity tests are performed by changing the input signals. In order to estimate the maximum linearity range of the sample, the input signals are set larger than those in above sensitivity tests. The observed scale factor behavior is shown in Table I. Here the scale factor calculated at smallest applied signal is defined as 100% level. As the input signal

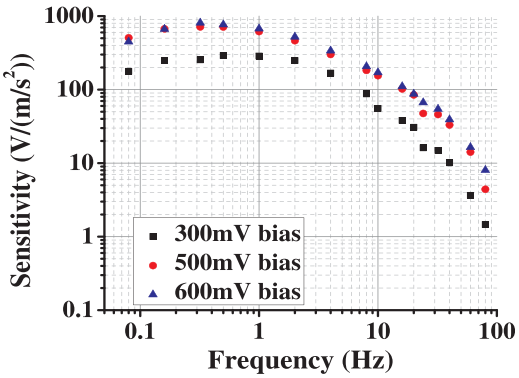

FIG. 3. Measurement results of sensitivity frequency response of fabricated micro MET seismometer in different bias conditions.

TABLE I. Scale factor vs. input acceleration (mm/s^2) at 8 Hz.

Acceleration	1.5	6	12	30	60	120
Scale factor	100%	98.8%	98.1%	5.8%	6.8%	5.8%

increases, the scale factor decreases very slowly for relatively small inputs. Finally, a very non-linear behavior is observed at input signals higher than ~2mg at 8 Hz, where a dramatic drop of scale factor can be seen. Based on Table I, the linear range for the sensor is limited to 2 mg level. Practically, the linear range can be expanded by 1–2 orders of magnitude without any changes in the sensing cell design if a negative feedback mechanism is implemented.

There are several contributors to the self-noise of the micro MET seismometer. One of the major contributors is the thermo-hydrodynamic self-noise which is generated from the fluctuations of the pressure difference on both sides of the channel. This noise in the unit of input acceleration is frequency independent[15]

$$\langle a^2 \rangle_\omega = \frac{2k_B T R_h}{\rho^2 L^2}, \quad (6)$$

where T is the absolute temperature and k_B is Boltzmann's constant. Under laminar flow condition, R_h has an expression of

$$R_h = \frac{1}{N}\frac{8\mu l}{\pi r^4}. \quad (7)$$

Where r is the radius of the circular cross-section of the channel, μ is the viscosity of the fluid, N is the number of channels, and l is the length of the sensing core. By scaling the inter-electrode spacing d down to 1μm, l is decreased to 5.8μm from several millimeters in traditional device, which reduces R_h significantly, thereby lower the thermo-hydrodynamic self-noise. Other contributors to the self-noise include convective noise,[16] hydrodynamic thermal noise produced by the circular flows of the liquid,[15] geometrical noise, shot noise, and noise of the signal conditioning electronics. Self-noise testing of the micro MET seismometer is conducted in the underground vault. The tested self-noise spectrum for a single-50μm diameter-channel device and a $5-50\mu$m diameter-channel device are shown in Fig. 4, both

This article is copyrighted as indicated in the article. Reuse of AIP content is subject to the terms at: http://scitation.aip.org/termsconditions. Downloaded to IP: 129.219.247.33 On: Mon, 09 Feb 2015 02:58:34

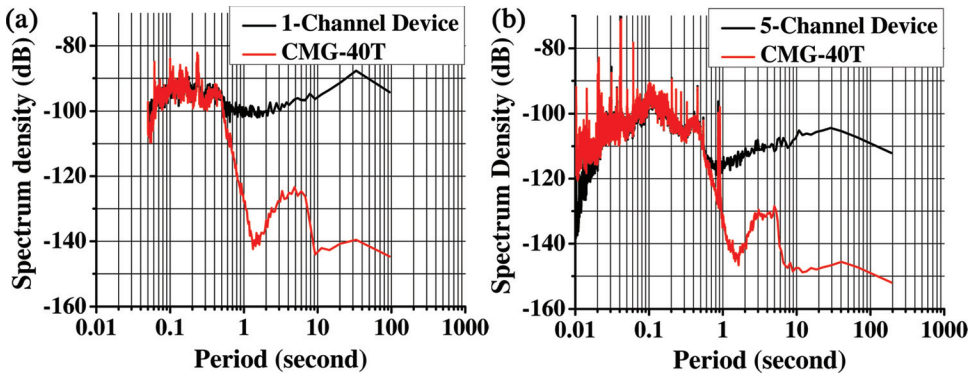

FIG. 4. Self-noise spectrum density of fabricated (a) single-50μm diameter-channel device (b) 5−50μm diameter-channel device.

in comparison with a commercialized CMG-40T seismometer (Guralp Systems Ltd.). The conclusions can be drawn from the data presented: (i) the self-noise achieves $-100\text{dB}(1.0\mu g/\sqrt{Hz})$ at 1 Hz for the single-channel device.[9] The 5-channel device whose hydrodynamic resistance is 5 times lower than that of single-channel one shows approximately a 5-fold (15 dB) decrease in self-noise, with $-115\text{dB}(0.18\mu g/\sqrt{Hz})$ at 1 Hz; (ii) the noise spectrum is not flat in the frequency range and demonstrates at low-frequency end of the spectrum the behavior close to 1/*f* type; (iii) the noise level is higher than predicted by Eq. (6) at all frequencies. Such behavior is consistent with the assumption that the primary contributor to the self-noise for the tested sample is 1/*f* noise of the electronic components.

In conclusion, a prototype of micromachined MET seismometer suitable for planetary exploration is developed. The transfer functions of the mechanical and electrochemical subsystems of the device are investigated. MET seismometer has a similar mechanical dynamic behavior as a solid-state seismometer, but no moving mechanics subject to possible damage, which makes the performance more reliable and enables inherent ability to withstand high shock forces. Typical parameters that influence the dynamic behavior of the MET seismometer include resonant frequency of the fluid and diffusion frequency of the electrochemical cell. Thanks to the MEMS microfabrication techniques, the diffusion frequency above which the sensitivity amplitude frequency response starts to decay significantly is increased by decreasing the inter-electrode distance down to 1μm. The seismometer can thus provide sufficiently large response within a wide frequency range. This is experimentally validated by measuring the sensitivity frequency response of the fabricated and assembled micro MET seismometer under varied external excitations in both short and long period. A second advantage of scaling down the inter-electrode spacing is its contribution to noise reduction. The performance can be further optimized for specific applications by adjusting the geometry of the sensing cell and the hydrodynamic resistance.

The work was majorly supported by NASA-PIDDP-NNX10AL25G (USA) and partially supported by Russian Foundation for Basic Researches (Grant No. 12-07-12057-ofi-m).

[1]D. L. Anderson, W. F. Miller, G. V. Latham, Y. Nakamura, M. N. Toksoz, A. M. Dainty, F. K. Duennebier, A. R. Lazarewicz, R. L. Kovach, and T. C. D. Knight, J. Geophys. Res. **82**, 4524–4546, doi:10.1029/JS082i028p04524 (1977).
[2]T. Hopf, S. Kumar, W. J. Karl, and W. T. Pike, Adv. Space Res. **45**, 460 (2010).
[3]P. Lognonne, D. Giardini, B. Banerdt, J. Gagnepain-Beyneix, A. Mocquet, T. Spohn, J. F. Karczewski, P. Schibler, S. Cacho, W. T. Pike, C. Cavoit, A. Desautez, J. Pinassaud, D. Breuer, M. Campillo, P. Defraigne, V. Dehant, A. Deschamp, J. Hinderer, J. J. Lvque, J. P. Montagner, and J. Oberst, Planet. Space Sci. **48**, 1289–1302 (2000).
[4]W. T. Pike, I. M. Standley, W. J. Karl, S. Kumar, T. Semple, S. J. Vijendran, and T. Hopf, in *International Solid-State Sensors, Actuators and Microsystems Conference* (Transducers 2009), 2009, Denver, CO, USA.
[5]P. Lognonne, Annu. Rev. Earth Planet. Sci. **33**, 571–604 (2005).
[6]V. A. Kozlov, V. M. Agafonov, J. Bindler, and A. V. Vishnyakov, in Proceedings of the 2006 National Technical Meeting of the Institute of Navigation, Monterey, CA, USA, 2006, pp. 650–655.
[7]W. He, D. Chen, G. Li, and J. Wang, Key Eng. Mater. **503**, 75–80 (2012).
[8]G. Li, D. Chen, W. He, and J. Wang, Key Eng. Mater. **503**, 61–66 (2012).
[9]H. Huang, B. Carande, R. Tang, J. Oiler, D. Zaitez, V. Agafonov, and H. Yu, in 26th IEEE International Conference on Micro Electro Mechanical Systems (MEMS 2013), Taipei, Taiwan, 2013, pp. 629–632.
[10]V. G. Krishtop, V. M. Agafonov, and A. S. Bugaev, Russ. J. Electrochem. **48**, 746–755 (2012).
[11]L. D. Landau and E. M. Lifshitz, *Theory of Elasticity* (Oxford, 1986).
[12]Z. Sun and V. M. Agafonov, Electrochim. Acta **55**, 2036–2043 (2010).
[13]C. W. Larcam, J. Acoust. Soc. Am. **37**, 664 (1965).
[14]V. A. Kozlov and M. V. Safonov, Russ. J. Electrochem. **40**, 460–462 (2004).
[15]V. A. Kozlov and M. V. Safonov, Tech. Phys. **48**, 1579 (2003).
[16]V. M. Agafonov and D. L. Zaitsev, Tech. Phys. **55**, 130–136 (2010).

This article is copyrighted as indicated in the article. Reuse of AIP content is subject to the terms at: http://scitation.aip.org/termsconditions. Downloaded to IP: 129.219.247.33 On: Mon, 09 Feb 2015 02:58:34